

THIN FILM CRACKING AND THE ROLES OF SUBSTRATE AND INTERFACE

T. YE†, Z. SUO and A. G. EVANS

Materials Department, University of California, Santa Barbara,
CA 93106-5050, U.S.A.

(Received 6 August 1991; in revised form 13 March 1992)

Abstract—Cracks in thin films caused by residual tension are examined. Attention is focused on film cracking, subject to either interface debonding or substrate cracking. For crack channeling along the film, the driving force is found to depend on the channel cross-section, as governed by the fracture properties of the interface and the substrate, in addition to known effects of film thickness, residual stress and elastic moduli. The critical film thickness needed to avoid cracking is determined to be lower if the crack extends into the substrate. Conditions for thin film spalling and constrained debonding are prescribed. Finally, the *T*-stress is used to account for crack branching in substrates.

1. INTRODUCTION

Thin films deposited on a substrate are usually subject to residual stress, with a misfit strain ϵ_0 . For example, if the thermal expansion coefficient of the film differs from that of the substrate, the misfit strain is biaxial, having magnitude

$$\epsilon_0 = (b_f - b_s)\Delta T, \quad (1)$$

where ΔT is the temperature drop and b the thermal expansion coefficient; the subscripts *f* and *s* indicate film and substrate, respectively. The misfit stress in the film is also biaxial, with magnitude

$$\sigma_0 = \epsilon_0 E_f / (1 - \nu_f), \quad (2)$$

where E_f is the Young's modulus and ν_f the Poisson's ratio. The residual stress is tensile when the thermal expansion coefficient for the film is larger than for the substrate, and is given explicitly by eqn (2) when the film is much thinner than the substrate. Thin films in residual tension are considered in this paper.

Many cracking patterns in film-substrate systems have been observed and analysed (Evans *et al.*, 1988; Hutchinson and Suo, 1992). A crack nucleates from a flaw either in the film or at the edge, and propagates both towards the interface and laterally through the film. Depending on the material, the crack may stop at the interface (Fig. 1a), penetrate into the substrate (Fig. 1b), or bifurcate onto the interface (Fig. 1c). These cracks then channel laterally. After the channel length exceeds a few times the film thickness h , a *steady state* is reached, wherein the entire front and the cross-section in the wake maintain their shape as the crack advances. When the steady-state channel extends by unit length, the potential energy decreases by (Suo, 1990; Ho and Suo, 1991)

$$\mathcal{U} = \frac{\sigma_0}{2} \int_0^h \delta(x) dx, \quad (3a)$$

† Now at Stewart & Stevenson Services, Inc., Gas Turbine Products Division, 164 15 Jacintport Blvd, Houston, TX 77015, U.S.A.

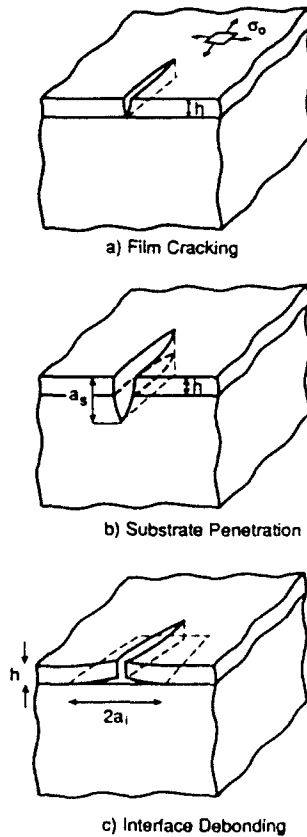


Fig. 1. (a) A channeling crack within a thin film. (b) A channeling crack penetrating into the substrate. (c) A channeling crack with interface debonding.

or by (Gille, 1985; Hu and Evans, 1988)

$$\mathcal{U} = \int \mathcal{G}(a) da, \quad (3b)$$

where $\delta(x)$ is the separation of the cracked film in the wake, $\mathcal{G}(a)$ is the energy release rate of a plane strain crack, and the integration in eqn (3b) is over all cracks in the cross-section of the wake.

Previous studies have assumed that the channel bottom is a sharp crack front lying on the interface (Fig. 1a). However, in practice a film crack may either extend into the substrate (Fig. 1b) or bifurcate along the interface (Fig. 1c), depending upon the relative fracture energies of thin film, substrate and interface. Such microscopic features relax the constraint of the system and increase the separation $\delta(x)$ which, in turn, increases the driving force \mathcal{U} . Consequently, the loss of constraint lowers the critical residual stress needed to drive the channel crack. Explicit determination of these effects is the subject of this article.

Consider an ideally constrained channel in the film (Fig. 1a). The potential energy decrease for the channel to extend unit length, \mathcal{U} , equals the energy released at the channel front, $h \mathcal{G}_{ss}$. Dimensional arguments lead to

$$h \mathcal{G}_{ss} = \mathcal{U} = (\sigma_0^2 h^2 / \bar{E}_f) \Sigma, \quad (4)$$

where $\bar{E}_f = E_f / (1 - \nu_f^2)$, and Σ is dimensionless and depends on elastic mismatch, as calculated by Beuth (1992) for the channel confined in the film.

Table 1. Fracture energies for typical film/substrate combinations

| Material | Fracture energy (Jm ⁻²) | Film/substrate† |
|--------------------------------|-------------------------------------|-----------------|
| Si | 6 | F, S |
| GaAs | 2-4 | F, S |
| SiO ₂ | 6 | F |
| SiC | 20 | F |
| Si ₃ N ₄ | 10-40 | F |
| Al ₂ O ₃ | 10-30 | S |
| Cu | 10 ⁴ | F |
| Al | 10 ⁴ | F |
| Ni | 10 ⁴ | F, S |
| Polyimide | 10 ³ | F |

† F refers to film, S refers to substrate.

Let Γ_f be the fracture energy of the film, and define a non-dimensional cracking number, Ω_c , as

$$\Omega_c = \sigma_0^2 h / \bar{E}_f \Gamma_f \tag{5}$$

The channel grows if $\mathcal{G}_{cs} = \Gamma_f$. Consequently, for the ideally constrained channel to grow, $\Omega_c = 1/\Sigma$. Once Ω_c has been established, it defines a critical film thickness below which film cracking is prohibited

$$h_c = \Omega_c (\bar{E}_f \Gamma_f / \sigma_0^2) \tag{5a}$$

Determination of Ω_c is the principal objective of this paper.

The material properties that dominate the conditions for film cracking, through their influence on the magnitude of Ω_c , are the system fracture energies and the elastic mismatch parameters. The relevant fracture energies Γ are Γ_i/Γ_f and Γ_s/Γ_f , where the subscripts i, f and s refer to the interface, film and substrate, respectively. Typical values for Γ_f and Γ_i are indicated in Table 1 for substrate and film combinations of technological interest. The interface fracture energy Γ_i is sensitive to details regarding the substrate surface, as well as the film deposition and post annealed processes. Values in the range 01-100 JM⁻² have been measured for various systems (Reimanis *et al.*, 1991 ; Evans *et al.*, 1990).

2. PLANE STRAIN PROBLEMS

The elastic mismatch is characterized by the two Dundurs' parameters

$$\alpha = \frac{(1 - \nu_s)/\mu_s - (1 - \nu_f)/\mu_f}{(1 - \nu_s)/\mu_s + (1 - \nu_f)/\mu_f}, \quad \beta = \frac{1}{2} \frac{(1 - 2\nu_s)/\mu_s - (1 - 2\nu_f)/\mu_f}{(1 - \nu_s)/\mu_s + (1 - \nu_f)/\mu_f} \tag{6}$$

where μ is the shear modulus and ν the Poisson's ratio. For typical film/substrate combinations, α and β tend to be interrelated, such that $\beta \approx \alpha/4$ (Evans *et al.*, 1990) with α ranging between 0 and 0.7. In the computational results reported below, $\nu_f = \nu_s = \frac{1}{3}$ (equivalently, $\beta = \alpha/4$).

The plane strain problems pertaining to the *wake of the channel*, shown in the insets of Fig. 2, provide the information needed to determine the potential energy decrease for channel cracking, \mathcal{U} . Each material is taken to be isotropic and linearly elastic, the substrate is semi-infinite and, by using Eshelby arguments, the stress intensity induced by the misfit stress must equal that induced by an applied traction of the magnitude.

For linear elastic problems, the plane strain energy release rate \mathcal{G} is quadratic in the residual stress and dimensional considerations show that

$$\mathcal{G} = (\sigma_0^2 h / \bar{E}_f) \omega \tag{7}$$

where ω is a dimensionless number depending on a/h , α and β . A few mathematical considerations capture the main features of the solution, as follows.

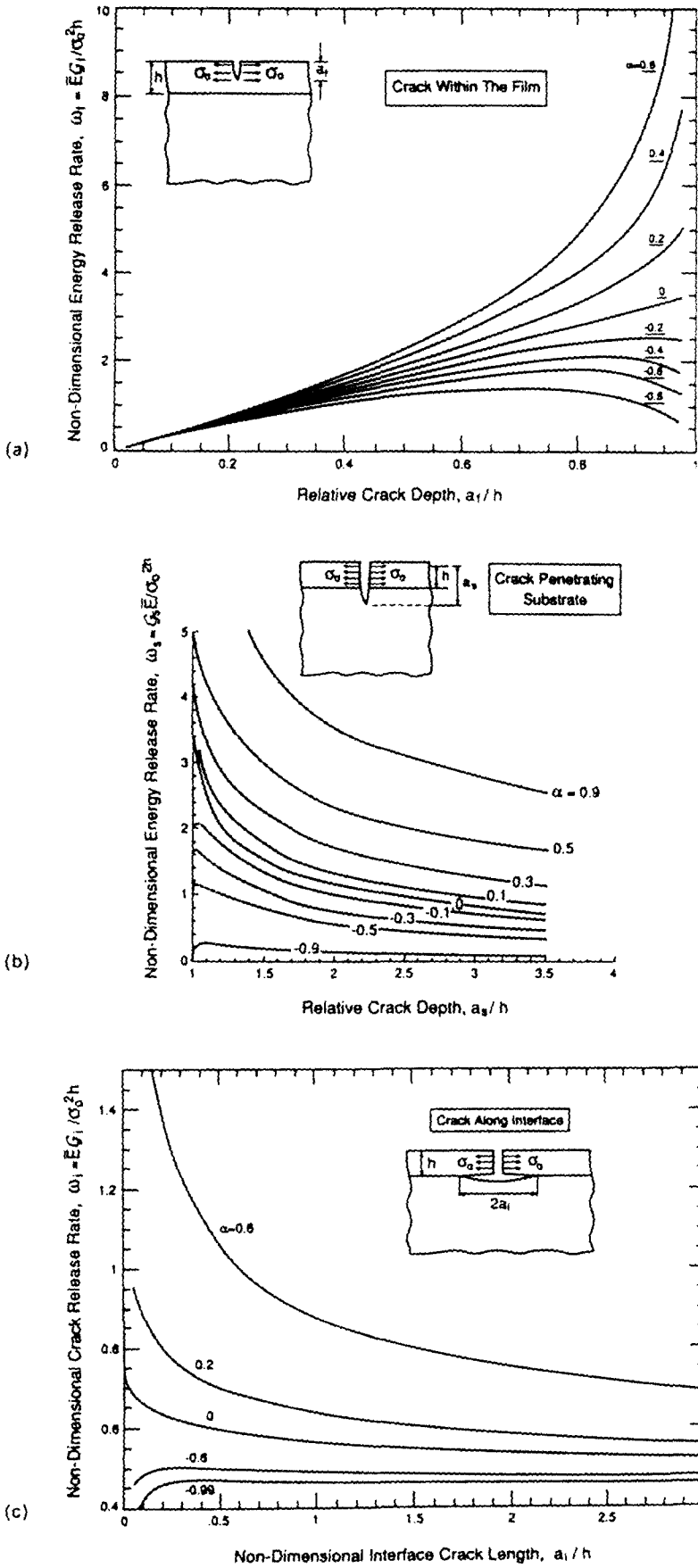


Fig. 2. Energy release rate for cracks under plane strain conditions. (a) Crack tip in the film. (b) Crack tip in the substrate. (c) Interface crack.

The stress field for a crack perpendicular to the interface, with the tip at the interface, is given by Zak and Williams (1963). The singular term is

$$\sigma_{ij} \sim \tilde{K} r^{-s} f_{ij}(\theta), \tag{8}$$

where (r, θ) is the polar coordinate centered at the tip, and f_{ij} are dimensionless angular distributions. The scaling factor, \tilde{K} , is analogous to the regular stress intensity factor, but having different dimensions [stress] [length]^s. The exponent s ($0 < s < 1$) is the root to

$$\cos(s\pi) - 2 \left[\frac{\alpha - \beta}{1 - \beta} \right] (1 - s)^2 + \left[\frac{\alpha - \beta^2}{1 - \beta^2} \right] = 0. \tag{9}$$

Table 1 lists s for given values of α . Dimensionality and linearity require that

$$\tilde{K} \sim \sigma h^s, \tag{10}$$

with the pre-factor dependent on α and β only.

Now consider a crack perpendicular to the interface, but with the crack tip either in the film or in the substrate (Figs 2a, b). As $a/h \rightarrow 1$, the stress field far from the small ligament $|h - a|$ behaves as if the crack tip were on the interface and is governed by \tilde{K} . At the crack tip, however, the stress field is square root singular and is scaled by the regular stress intensity factor K . Linearity requires that

$$K \sim \tilde{K} |h - a|^{1/2-s}. \tag{11}$$

Combination of eqns (10) and (11) gives

$$K/\sigma_0 \sqrt{h} \sim \begin{cases} (1 - a/h)^{1/2-s}, & a/h \rightarrow 1^- \\ (1 - h/a)^{1/2-s}, & a/h \rightarrow 1^+ \end{cases} \tag{12}$$

2.1. Crack tip in the film

For a crack tip in the film (Fig. 2a), Beuth (1991) has shown that, subject to $\mathcal{G}_f = K^2/\tilde{E}_f$,

$$\omega_f = 3.951 \eta_f (1 - \eta_f)^{1-2s} (1 + \lambda_1 \eta_f)^2, \tag{13}$$

where ω_f is the dimensionless number defined in eqn (7), $\eta_f = a_f/h$ and λ_1 is a fitting parameter to the full numerical solution (Table 2). The pre-factor is chosen such that, as $\eta_f \rightarrow 0$, eqn (13) approaches the classical solution of an edge crack in a semi-infinite homogeneous plane. Notice that the normalized energy release rate ω_f increases with α , confirming the known behavior that a compliant substrate attracts cracks more than a stiff substrate.

2.2. Crack tip in the substrate

For a crack that penetrates into the substrate (Fig. 2b) by using $\mathcal{G}_s = K^2/\tilde{E}_s$, our finite element results can be expressed as

$$\omega_s = \frac{4\pi}{\pi^2 - 4} (\tilde{E}_f/\tilde{E}_s) \eta_s [\sin^{-1}(1/\eta_s) (1 - \eta_s^{-1})^{1-2s} (1 + \lambda_2/\eta_s)]^2, \tag{14}$$

Table 2. ($v_f = v_s = \frac{1}{2}$, or $\beta = \alpha/4$)

| | | | | | | | | | | | |
|-------------|---------|---------|---------|---------|---------|--------|--------|--------|--------|--------|---------|
| α | -0.99 | -0.8 | -0.6 | -0.4 | -0.2 | 0 | 0.2 | 0.4 | 0.6 | 0.8 | 0.99 |
| s | 0.312 | 0.350 | 0.388 | 0.425 | 0.462 | 0.500 | 0.542 | 0.591 | 0.654 | 0.744 | 0.940 |
| λ_1 | -0.0894 | -0.0784 | -0.0627 | -0.0437 | -0.0224 | 0 | 0.0215 | 0.0389 | 0.0465 | 0.0335 | -0.0257 |
| λ_2 | 1.087 | 0.711 | 0.429 | 0.211 | 0.0201 | -0.136 | -0.296 | -0.440 | -0.584 | -0.708 | -0.962 |
| λ_3 | 2.220 | 1.951 | 1.615 | 1.282 | 0.957 | 0.496 | 0.660 | 0.666 | 0.796 | 1.268 | |
| λ_4 | 2.391 | 2.570 | 2.594 | 2.392 | 2.017 | 1.336 | 1.217 | 0.918 | 0.694 | 0.521 | |

where ω , is the dimensionless number defined in eqn (7), $\eta = a_s/h$, and the fitting parameter λ_2 is listed in Table 2. The pre-factor ensures that, as $\eta_s \rightarrow \infty$ eqn (14) approaches the solution of an edge crack in a semi-infinite plane loaded by a pair of point forces (Tada *et al.*, 1985). Since the residual stress is localized in the film, the energy release rate decreases rapidly as the plane strain crack extends into the substrate.

2.3. Interface crack

When the crack extends along the interface (Fig. 2c), even though stresses are oscillatory at an interface crack tip, the energy release rate \mathcal{G}_i still has the usual interpretation. Finite element calculation provides the following approximation:

$$\omega_i = \frac{1}{2} \left(\frac{\eta_i}{1 + \eta_i} \right)^{1-2\alpha} [1 + \lambda_3 \exp(-\lambda_4 \sqrt{\eta_i})], \quad (15)$$

where ω_i is the dimensionless number defined in eqn (7) and $\eta_i = a_i/h$. The two parameters, λ_3 and λ_4 , used to fit the finite element solutions are listed in Table 2. The pre-factor ensures that the solution is exact as $\eta_i \rightarrow \infty$. For systems having films stiffer than substrates ($\alpha > 0$), ω_i monotonically decreases to a constant level, $\omega_i = 0.5$. For such systems, the interface debonds, unless the crack can either blunt or extend into the substrate. For more compliant films ($\alpha < 0$), a maximum ω_i exists, suggesting a condition wherein debonding could not occur provided that the interface toughness exceeds a critical level.

3. CHANNEL CRACKS

3.1. Brittle substrates

When the substrate is brittle, the crack in the film may penetrate into the substrate (Fig. 1b). Thus, \mathcal{U} can be obtained by substituting eqns (13) and (14) into eqn (3b) to give

$$\mathcal{U} \frac{E_f}{\sigma_0^2 h^2} \equiv \Sigma = \int_0^1 \omega_f d\eta_f + \int_1^{a_s/h} \omega_s d\eta_s. \quad (16)$$

For a unit advance of the channel, the potential energy is balanced by the energy needed to create crack surfaces

$$\mathcal{U} = h\Gamma_f + (a_s - h)\Gamma_s, \quad (17)$$

where Γ_f and Γ_s are fracture energies for the film and substrate, respectively. At the bottom of the channel, the energy release rate must equal the fracture energy of the substrate,

$$\mathcal{G} = \Gamma_s. \quad (18)$$

Equations (17) and (18) can be rewritten in nondimensional forms

$$\Omega_c = [1 + (\Gamma_s/\Gamma_f)(\eta_s^* - 1)]/\Sigma \quad (19a)$$

and

$$\omega_s \Omega_c = \Gamma_s/\Gamma_f, \quad (19b)$$

where Ω_c is defined by eqn (5). Equations (19a, b) can be solved to give the channel depth into the substrate, $\eta_s^* [= (a_s/h)^*]$, and the critical cracking number, Ω_c , as a function of both Γ_s/Γ_f and the Dundurs' parameter, α . Both equations are nonlinear in η_s , since Σ and ω_s depend on η_s .

It is apparent from Fig. 3a that the crack depth into the substrate increases either as the relative substrate fracture energy, Γ_s/Γ_f , decreases or as α increases. The cracking

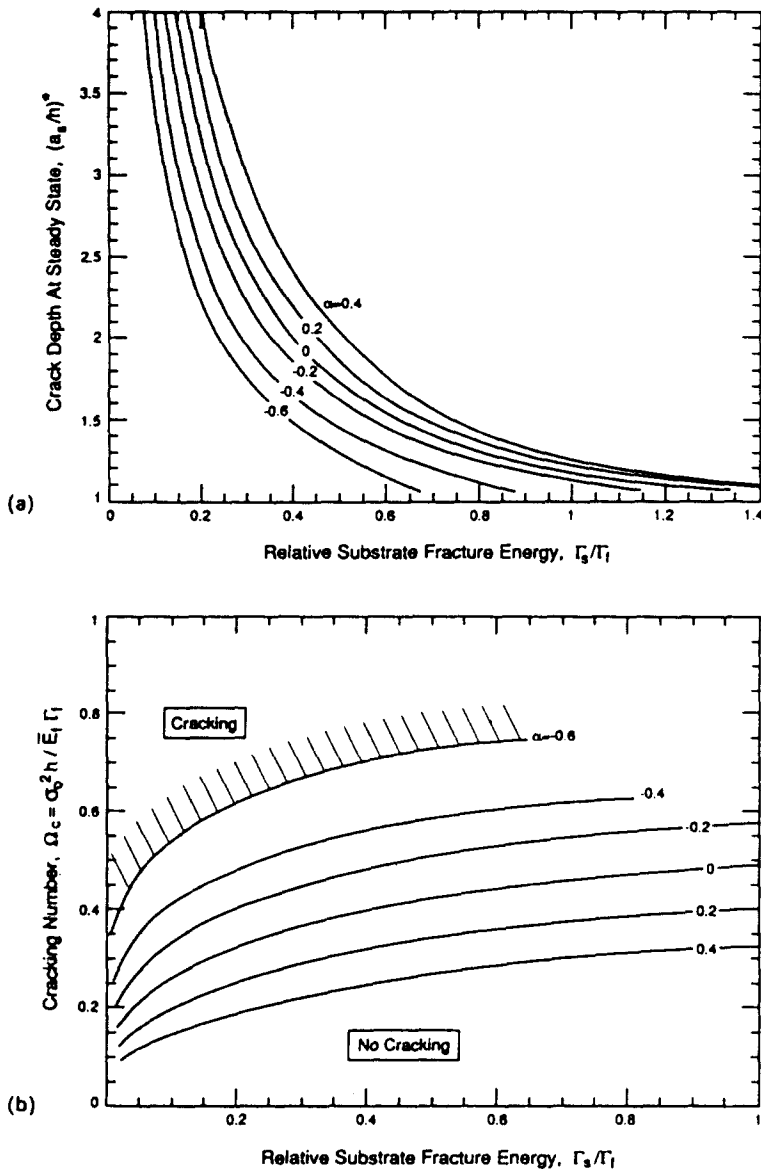


Fig. 3. The effect of substrate fracture energy and elastic mismatch on (a) the steady-state crack depth and (b) the film cracking and non-cracking regimes, expressed through the cracking number, Ω_c .

number Ω_c decreases as small Γ_s/Γ_f (Fig. 3b), reducing the critical film thickness, h_c . However, it is also of importance to note that Ω_c is essentially invariant when $\Gamma_s/\Gamma_f \gg 1$. This is consistent with the prediction that crack penetration into film is negligible when $\Gamma_s/\Gamma_f \gg 1$ (Fig. 3a). Consequently, the substrate fracture properties are *only important when the substrate has appreciably less toughness than the film*.

3.2. Weak interfaces

Denote Γ_i as the fracture energy of the interface at the phase angle pertinent to interface debonding [52° when film and substrate have similar elastic constraints; see Fig. 53 in Hutchinson and Suo (1992)]. The non-dimensional energy release rate for an interface crack quickly approaches an asymptotic value, $\omega_i = 0.5$ (Fig. 2c). For practical purposes, this prescribes the critical cracking number defined in eqn (5) as

$$\Omega_c = 2\Gamma_i/\Gamma_f. \tag{20}$$

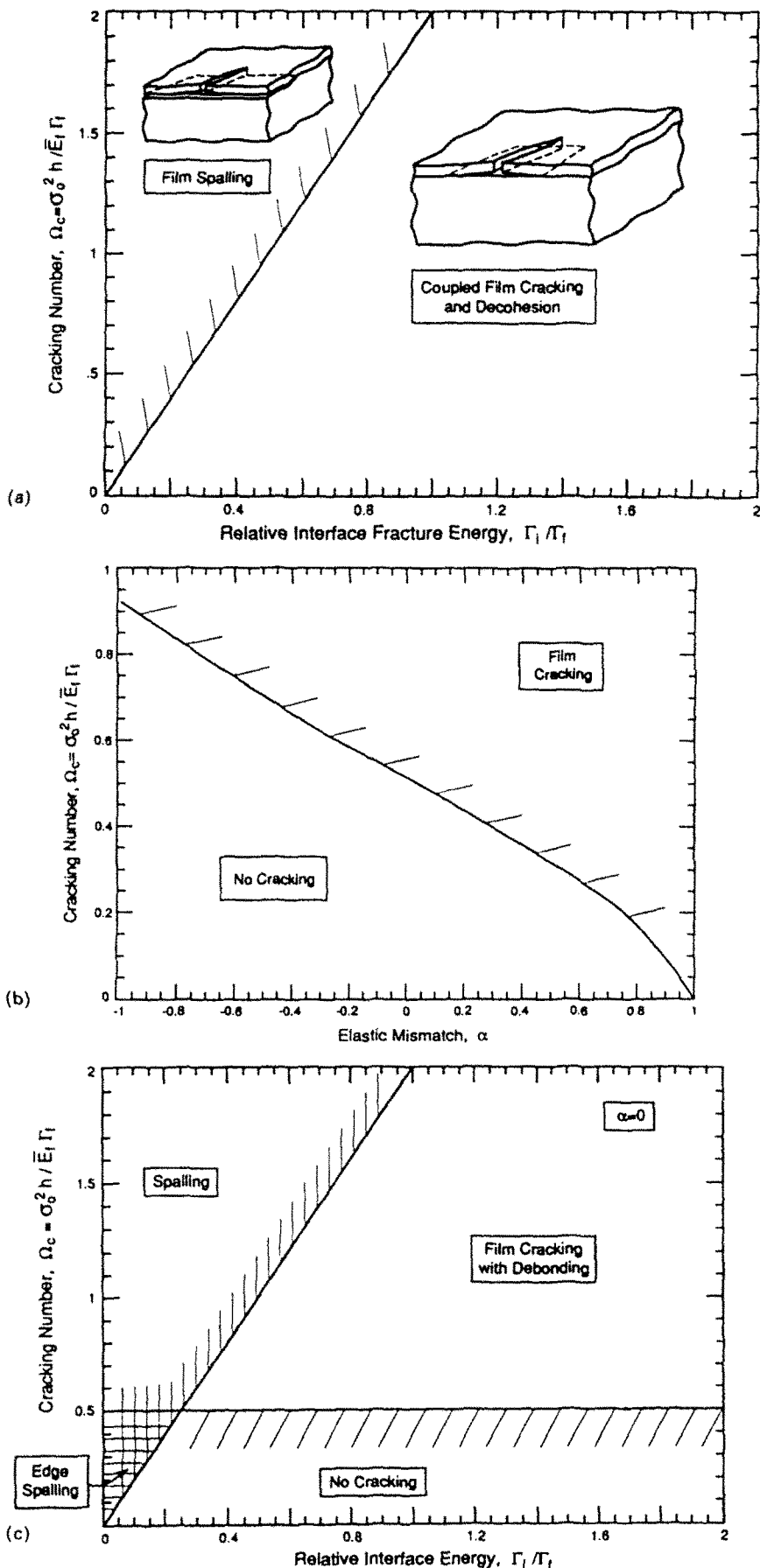


Fig. 4. Cracking regimes when interface debonding occurs. (a) the spalling regime, (b) the non-cracking regime, (c) a cracking map.

The interpretation of this result is as follows. For $\Omega_c > 2\Gamma_i/\Gamma_f$, the debond extends without limit and the entire film spalls off as the crack extends across the film, (Fig. 4a). This condition does not depend on the Dundurs' parameter, α .

Another limit coincides with the condition for the avoidance of cracking. This limit arises when $\eta_i = 0$ (Beuth, 1992)

$$\Omega_c = \frac{1}{\int_0^1 \omega_r d\eta_r} \tag{21}$$

This condition depends on α (Fig. 4b). A map that combines the above information is shown in Fig. 4c for the case $\alpha = 0$. The area indicated by edge cracking indicates that thin film cracking is avoided, but Γ_i is so low that interface debonds from the edge of the film. It is noted that constrained debonding does not reduce Ω_c appreciably, so that Fig. 4b is sufficient for practical purposes.

4. CRACK BRANCHING IN THE SUBSTRATE

After a crack penetrates into a brittle substrate, it bifurcates (Drory and Evans, 1990) (Fig. 5). To account for this phenomenon, the concept of the T -stress is used. For a mode I crack, the Williams expansion defines T -stress as

$$\sigma_{ij}(r, \theta) = \frac{K}{\sqrt{2\pi r}} f_{ij}(\theta) + T\delta_{ij}, \tag{22}$$

where T is the stress acting parallel to the crack. A crack in an isotropic, homogeneous, brittle solid normally selects a trajectory with mode I loading. The crack perpendicular to the interface, with tip in the substrate, is indeed under mode I. According to Cotterell and Rice (1980), a mode I crack is directionally stable if $T < 0$, but unstable if $T > 0$. With this concept in mind, the T -stress after a crack penetrates into the substrate was computed using finite elements (Fig. 5). It is apparent that conditions exist near the interface with $T > 0$. Cracks in the substrate near the interface thus appear to be unstable. The observed bifurcation may be plausibly explained by this effect. Noticing that the singular term in (22) vanishes in crack flanks and, in particular, $f_{xx}(\pm\pi) = 0$, we compute σ_{xx} using finite element along the flanks, near the crack tip, which approaches T . Fine meshes at the crack tip are

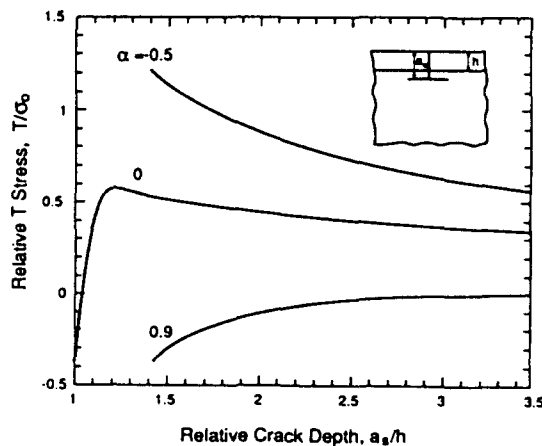


Fig. 5. The T -stress as a function of substrate crack depth for various levels of elastic mismatch. The crack branches when $T > 0$.

used which are varied and refined to ascertain mesh insensitivity [see Sham (1991) for more sophisticated methods for computing T -stress].

Acknowledgements—This investigation is supported by the ONR/URI contract 8-482491-25910-3. ZS is in addition supported by NSF grant MSS-9011571. The finite element computations were performed using ABAQUS. We thank the reviewers for several suggestions.

REFERENCES

- Beuth, J. L. (1992). Cracking of thin bonded films in residual tension. *Int. J. Solids Structures* **29**, 1657–1675.
- Cotterell, B. and Rice, J. R. (1980). Slightly curved or kinked cracks. *Int. J. Fract.* **16**, 155–169.
- Drory, M. D. and Evans, A. G. (1990). Experimental observation of substrate fracture caused by residual stressed films. *J. Am. Ceram. Soc.* **73**, 634–638.
- Evans, A. G., Drory, M. D. and Hu, M. S. (1988). The cracking and decohesion of thin films. *J. Mater. Res.* **3**, 1043–1049.
- Evans, A. G., Rühle, M., Dalgleish, B. J. and Charalambides, P. G. (1990). The fracture energy of bimaterial interface. *Mat. Sci. Engng A* **126**, 53–64.
- Gille, G. (1985). Strength of thin films and coatings. In *Current Topics in Materials Science* (Edited by E. Kaldis), Vol. 12. North Holland, Amsterdam.
- Ho, S. and Suo, Z. (1991). Tunnelling cracks in constrained layers (submitted).
- Hutchinson, J. W. and Suo, Z. (1992). Mixed mode cracking in layered materials. *Adv. Appl. Mech.* **29**, 63–191.
- Hu, M. S. and Evans, A. G. (1988). The cracking and decohesion of thin films on ductile substrates. *Acta metall.* **37**, 917–259.
- Reimanis, I. E., Dalgleish, B. J. and Evans, A. G. (1991). The fracture resistance of a model metal/ceramic interface. *Acta Metall. Mater.* **39**, B133–B3142.
- Sham, T.-L. (1991). The determination of the elastic T -term using higher order weight functions. *Int. J. Fract.* **48**, 81–102.
- Suo, Z. (1990). Failure of brittle adhesive joints. *Appl. Mech. Rev.* **43**, S276–S279.
- Tada, H., Paris, P.C. and Irwin, G. R. (1985). *The Stress Analysis of Cracks Handbook*. Del. Research, St Louis, Mo.
- Zak, A. R. and Williams, M. L. (1963). Crack point stress singularities at a bi-material interface. *Appl. Mech.* **30**, 142–143.